

# Engineering *Synechococcus elongatus* PCC 7942 for Continuous Growth under Diurnal Conditions

Jordan T. McEwen, Iara M. P. Machado, Michael R. Connor,\* Shota Atsumi

Department of Chemistry, University of California, Davis, Davis, California, USA

*Synechococcus elongatus* strain PCC 7942 strictly depends upon the generation of photosynthetically derived energy for growth and is incapable of biomass increase in the absence of light energy. Obligate phototrophs' core metabolism is very similar to that of heterotrophic counterparts exhibiting diverse trophic behavior. Most characterized cyanobacterial species are obligate photoautotrophs under examined conditions. Here we determine that sugar transporter systems are the necessary genetic factors in order for a model cyanobacterium, *Synechococcus elongatus* PCC 7942, to grow continuously under diurnal (light/dark) conditions using saccharides such as glucose, xylose, and sucrose. While the universal causes of obligate photoautotrophy may be diverse, installing sugar transporters provides new insight into the mode of obligate photoautotrophy for cyanobacteria. Moreover, cyanobacterial chemical production has gained increased attention. However, this obligate phototroph is incapable of product formation in the absence of light. Thus, converting an obligate photoautotroph to a heterotroph is desirable for more efficient, economical, and controllable production systems.

All cyanobacteria are photosynthetic organisms that utilize light energy for the reduction of carbon dioxide. Certain characterized cyanobacteria have been shown to consume organic molecules for increased biomass in the presence of light, allowing photoorganoheterotrophy, while some cyanobacterial species have been shown to consume organic molecules regardless of light conditions. Other cultured cyanobacterial species are obligate photoautotrophs and as such lack the ability to consume fixed carbon compounds for increased biomass or energy. The precise causes for this inflexible trophic behavior are currently unknown; however, the matter is being studied (1, 2).

Two principal hypotheses have been proposed for obligate photoautotrophy among microorganisms. In some photoautotrophs, the lack of efficient uptake of essential substrates, especially sugars, into the cells may be the major reason for obligate photoautotrophy (3). However, impermeability of membranes to essential nutrients may not be the only factor in obligate photoautotrophy, considering that some photoautotrophs incorporate organic compounds into cellular carbon incapable of sustaining growth (4). It was hypothesized that a biosynthetic or degradative lesion in central metabolism might cause obligate photoautotrophy (5). An incomplete tricarboxylic acid (TCA) cycle may be a vital reason in some phototrophic microorganisms. Wood et al. found that most photoautotrophic organisms lack at least one of the three components of 2-ketoglutarate dehydrogenase complex causing an incomplete TCA cycle (2). However, more recently, it has been shown that two alternative enzymes, 2-oxoglutarate decarboxylase and succinic semialdehyde dehydrogenase, convert 2-oxoglutarate to succinate and functionally complete the TCA cycle in cyanobacteria (6). Thus, we hypothesize that efficient uptake of sugars is the major missing factor inhibiting heterotrophy in obligate photoautotrophic cyanobacteria.

Sugar transporters have been exploited to expand trophic behavior and to export valuable biosynthetic products in a variety of organisms (3, 4, 7–11). Zaslavskaja et al. engineered a eukaryotic alga, *Phaeodactylum tricornutum*, to thrive on exogenous glucose in the absence of light by introducing a gene encoding a glucose transporter from human erythrocytes (*Glut1* or *Hup1*) (3). The

*P. tricornutum* strain expressing the *Glut1* gene exhibited high growth rates in the presence of glucose. The cell density attained by the mutants exceeded that of the wild type by 15-fold (3). This result indicates that in some eukaryotic microalgae, the lack of efficient sugar uptake into the cells is a major reason for their obligate photoautotrophy.

Several investigations to examine obligate photoautotrophy in cyanobacteria with recombinant sugar transporter strategies have been attempted, yet a conclusive determination of the causes of photoautotrophy has proven to be elusive. The *glcP* gene, encoding a glucose transporter from the heterotrophic cyanobacterium, *Synechocystis* sp. strain PCC 6803, has been expressed from a plasmid-based expression system in *Synechococcus elongatus* strain PCC 7942 but could not be maintained, while genomic integration led to glucose sensitivity (4). Additionally, the fructose transport and regulation system of filamentous *Anabaena variabilis* was introduced into the closely related photoautotrophic cyanobacterium *Anabaena* sp. strain PCC 7120, allowing limited fructose consumption and utilization only in the dark; however, it was later discovered that *Anabaena* sp. strain PCC 7120 can consume fructose without the introduction of heterologous genes (9, 10). Furthermore, *S. elongatus* has been engineered to successfully express a sugar transport system to export photosynthetic end products, such as glucose, fructose, and sucrose (7, 8). This work established the availability of all required enzymes for the synthesis of sugars from the metabolic products of the Calvin Benson Bassham cycle.

Received 29 October 2012 Accepted 26 December 2012

Published ahead of print 28 December 2012

Address correspondence to Shota Atsumi, satsumi@ucdavis.edu.

\* Present address: Michael R. Connor, Joule Unlimited, Bedford, Massachusetts, USA.

Supplemental material for this article may be found at <http://dx.doi.org/AEM.03326-12>.

Copyright © 2013, American Society for Microbiology. All Rights Reserved.  
doi:10.1128/AEM.03326-12

A reasonable assumption is that the reactions may be utilized in reverse for biomass increase from consumption of the corresponding sugar gradient.

Cyanobacteria are being considered as a platform for the conversion of renewable solar energy to biofuels (12–15). Current research supports the idea that cyanobacterial biosynthesis of fuels and industrial chemicals may be one of the most efficient approaches to reduce the need for imported petroleum and to minimize CO<sub>2</sub> emissions (16). Cyanobacteria are also a largely untapped source of natural products for drug discovery (17). However, many cyanobacteria are obligate photoautotrophs and thus incapable of increasing biomass in the absence of light energy. Here we focus on the consumption of sugars for the production of cyanobacterial biomass. Glucose is a central metabolite universally used for the storage of energy and is the most plentiful biomolecule on earth in the form of cellulose. Research is investigating efficient harvesting of glucose from cellulose as a feedstock for biofuel production. Sucrose is another important feedstock that is produced on the economic scale needed for common human consumption, as well as being utilized for biologically derived fuels and chemicals. Xylose is the final feedstock of interest addressed herein, plentiful as a major portion of hemicellulosic materials, and is a sugar not metabolized by humans. Probing the limitations of *S. elongatus* regarding the consumption of each of these common feedstocks gives a greater understanding of the more complex and general obligate photoautotrophic behavior, as well as aiding in the development of industrially relevant and versatile chemical-producing photosynthetic organisms.

## MATERIALS AND METHODS

**Reagents.** The chemicals glucose, fructose, sucrose, and xylose were obtained from Sigma-Aldrich (St. Louis, MO). Isopropyl-β-D-thiogalactopyranoside (IPTG) was obtained from Fisher Scientific (Hanover Park, IL). Phusion polymerase was purchased from NEB (Ipswich, MA). KOD polymerase was purchased from EMD4Biosciences (San Diego, CA). Spectinomycin was purchased from MP Biomedicals (Santa Ana, CA). Oligonucleotides were synthesized by Integrated DNA Technologies, Inc. (San Diego, CA).

**Culture conditions.** All cyanobacterial strains were grown in BG-11 medium (18) at 30°C with shaking at 100 rpm. All medium modifications are described below. Cultures were maintained in a custom cabinet with the dimensions 56 cm by 36 cm by 76 cm. This cabinet was outfitted with 2 compact fluorescent lamp (CFL) natural-spectrum bulbs from Verilux, rated at 26 W. Light fluence rates were 25 μE s<sup>-1</sup> m<sup>-2</sup>. Precultures for diurnal experiments were maintained for at least 72 h under diurnal lighting conditions to ensure proper circadian rhythm. All preculture was grown without the addition of sodium bicarbonate or any saccharide. Growth assays used a total volume of 10 ml of culture in 30-ml test tubes. All assays were conducted using biological triplicates. Cell growth was monitored by measuring the optical density at 730 nm (OD<sub>730</sub>) for each biological triplicate one time.

For growth assays using the *S. elongatus* strains, cells in exponential phase were diluted to an OD<sub>730</sub> of 0.2 in 10 ml BG-11 medium including 20 μg/ml spectinomycin and 0.1 mM IPTG, with all other modifications described below. Wild-type assays omitted spectinomycin.

Assays were examined for contamination by plating 50 μl of the culture from the final time point of every sample on Luria Bertani (LB) plates. In a few of the samples, slight contamination was detected (<20 colonies out of at least 10<sup>4</sup> cyanobacterial cells). To further quantify the contamination, bright-field microscopy was utilized. Cells were counted within a Petroff-Hausser counting chamber slide to ensure a constant volume throughout. Counting chambers were chosen randomly, and green cells versus colorless cells were tallied. For all reported results where contami-

TABLE 1 Strains and plasmids used in this study

Strain or plasmid	Relevant genotype	Source or reference
<b>Strains</b>		
AL257	<i>Synechococcus elongatus</i> PCC 7942 (wild type)	S. S. Golden
AL358	<i>P<sub>trc</sub></i> : <i>glcP</i> integrated at NSI	This work
AL360	<i>P<sub>trc</sub></i> : <i>GLUT1</i> integrated at NSI	This work
AL361	<i>P<sub>trc</sub></i> : <i>galP</i> integrated at NSI	This work
AL434	<i>P<sub>trc</sub></i> : <i>xyIE-xyIA-xyIB</i> integrated at NSI	This work
AL504	<i>P<sub>trc</sub></i> : <i>gfp</i> integrated at NSI	This work
AL505	<i>P<sub>trc</sub></i> : <i>galP-gfp</i> integrated at NSI	This work
AL535	Same as AL361 but Δ <i>glgC</i>	This work
AL536	Same as wild type but Δ <i>glgC</i>	This work
AL1030	<i>P<sub>trc</sub></i> : <i>cscK-cscB</i> integrated at NSI	This work
AL1067	<i>P<sub>trc</sub></i> : <i>xyIE</i> integrated at NSI	This work
<b>Plasmids</b>		
pAM2991	NSI targeting vector; <i>P<sub>trc</sub></i>	20
pBBR1MCS-5	Gm <sup>r</sup> ; broad-host-range vector	21
pSA69	P15A ori; Amp <sup>r</sup> ; <i>P<sub>LacO1</sub></i> : <i>alsS-ilyC-ilyD</i>	19
pAL18	Same as pAM2991 but <i>P<sub>trc</sub></i> : <i>GLUT1 lacI<sup>q</sup></i>	This work
pAL40	Same as pAM2991 but <i>P<sub>trc</sub></i> : <i>galP lacI<sup>q</sup></i>	This work
pAL46	Same as pAM2991 but <i>P<sub>trc</sub></i> : <i>glcP lacI<sup>q</sup></i>	This work
pAL61	Same as pAM2991 but <i>P<sub>trc</sub></i> : <i>gfp lacI<sup>q</sup></i>	This work
pAL63	Same as pAM2991 but <i>P<sub>trc</sub></i> : <i>gfp-galP lacI<sup>q</sup></i>	This work
pAL65	Same as pAM2991 but <i>P<sub>trc</sub></i> : <i>xyIE lacI<sup>q</sup></i>	This work
pAL70	Same as pAM2991 but <i>P<sub>trc</sub></i> : <i>xyIE-xyIA-xyIB lacI<sup>q</sup></i>	This work
pAL82	<i>glgC</i> knockout vector; Gm <sup>r</sup>	This work
pAL288	Same as pAM2991 but <i>P<sub>trc</sub></i> : <i>cscK-cscB lacI<sup>q</sup></i>	This work

nation was detected, green cells were greater than 99% of the culture ( $n \geq 500$ ).

**Plasmid construction.** All plasmids used in this work are described in Table 1. All primers used are listed in Table 2. All installed genes in this study are listed in Table 3.

The *galP*, *xyIE*, *xyIA*, and *xyIB* genes were amplified from *Escherichia coli* BW25113 genomic DNA. The *glcP* gene was amplified from *Synechocystis* sp. PCC 6803 genomic DNA (ATCC). *cscB* and *cscK* were amplified from genomic DNA of *E. coli* ATCC 700927 (ATCC). *galP* was amplified using the primers MC127 and MC128, digested with MfeI and BgIII, and then ligated with pAM 2991 digested with EcoRI and BamHI to create pAL40. *xyIE* was amplified using the primers JM05 and JM06, digested with EcoRI and BamHI, and ligated with pAM2991 digested with the same enzymes, creating pAL65. *xyIAB* was amplified using the primers JM07 and JM08 and digested with AvrII and BamHI, followed by ligation to similarly digested pAL65 to create pAL70. *glcP* was amplified using the primers MC170 and MC171, digested with BamHI and EcoRI, and ligated to similarly digested pAM 2991 to create pAL46. *cscB* and *cscK* were amplified using the primers JM55 and JM56, digested with EcoRI and BamHI, and ligated to similarly digested pAM2991 to create pAL289.

pAL82 was constructed in order to delete the *glgC* gene from the *S. elongatus* chromosome (see Fig. S1 in the supplemental material). The region for homologous recombination (590,459 to 593,751) was amplified from *S. elongatus* genomic DNA using the primers GR005 and GR006. The product was digested with XhoI and MluI and ligated with similarly digested pSA69 (19), creating pGR01. To clone the gentamicin resistance gene, pBBR1MCS-5 (21) was used as the PCR template with the primers IM573 and IM574. The PCR product was digested with SalI and NheI and ligated with pGR01 cut with the same enzyme, creating pAL82. The correct deletion of *glgC* was confirmed by PCR with the primers GR050 and IM581 and IM573 and GR015 (see Fig. S1B). The complete segregation of Δ*glgC* was confirmed by PCR using the primers IM171 and GR015 (see Fig. S1C).

**Transformation of *S. elongatus*.** Transformation of *S. elongatus* was performed as previously described (22). Strains were segregated several times by transferring colonies to fresh selective plates. Correct recombi-

TABLE 2 Oligonucleotides used in this study

Primer name	Sequence (5' → 3')
JM5	CCGGAATTC AATACCCAGTATAATTCCAGTTATATATTTTCGA
JM6	CGGGATCCATCCTAGGTTACAGCGTAGCAGTTTGTGT
JM7	CGCCTAGGAACTTTAAGAAGGAGATATACCATGCAAGCCTATTTTGACCAGCTCG
JM8	CGGGATCCTTACGCCATTAATGGCAGAAGTTGC
JM55	ATGGAATTCATGTCAGCCAAAGTATGGGT
JM56	GGATCCATTGGGACGTCACCTCCTATATTGCTGAAGGTACAGG
JM57	GAGGTGACGTCATGACGCAATCTCGATTGC
JM58	TAGAGGATCCTTAACCCAGTTGCCAGAGTG
JM66	ATGGAATTCATGGCACTGAATATTCCATT
MC127	CTAACAAATTGATGCCTGACGCTAAAAAACAGGGGCG
MC128	CTATAGATCTTTAATCGTGAGCGCCTATTTTCGCGCAGTT
MC186	CTATCTCGAGTTAATCGTGAGCGCCTATTTTCGCGCAGTT
MC187	CATGCCTGACGCTAAAAAACAGGGGCGGTCA
MC188	TTACGGCCGCTGCCACCGCCGCTACCGCCATCGTGAGCGCCTATTTTCGCGCAGTTTACG
MC189	ACGATGGCGGTAGCGGCGGTGGCAGCGGCCGTAAGGAGAAGAAGCTTTTCACTGGAGTT
MC190	CTTAGCATGCTTTGTATAGTTTCATCCATGCCATG
MC191	CTATGAATTCCGTAAGGAGAAGAAGCTTTTCACTGGAGTT
MC192	CTAAGGATCCTTAGCATGCTTTGTATAGTTTCATCCATGCCATG
IM171	GCTAGCAGCTCAGATTACGC
IM573	GGTGCTAGCCACCGTGGAACGGATGAAGG
IM574	CATTTTTGTGCGACGCCGGGAAGCCGATCTCG
IM581	GAGTAGGTGGCTACGTCTCC
GR005	CCGCTCGAGTACCAGCGATCCGTGTCCCTACTCG
GR006	CGAGCACGCGTCAATTGCCCTAAGACAGTTGTCTGC
GR015	CGCCGAAGTGTGTAACAGC
GR050	TAGTAACCTCCAGCCTTTTTTGCC

nants were confirmed by PCR and DNA sequencing to verify integration of targeting genes into the chromosome at NSI (see Fig. S2 in the supplemental material) (23). The strains used and constructed are listed in Table 1.

**Confocal microscopy.** All confocal microscope images were taken using the Olympus America FV1000 system located within the UCD NEAT Spectral Imaging Facility. A 488-nm laser was used for excitation of all mutants. The emission filter was set 500 nm to 600 nm. The pinhole aperture was set to 100  $\mu\text{m}$ . The laser percentage was set to 11.5%. Cells were placed in glass-bottom dishes for imaging.

**GFP assay on plate reader.** All green fluorescent protein (GFP) assays were done using a Microtek Synergy H1 plate reader (BioTek). BG-11 medium only was used as a blank, and excitation and emission wavelengths were set to 485 and 528 nm, respectively.

**Glucose and xylose consumption assays.** Glucose and xylose concentrations in the culture medium were measured using a high-performance liquid chromatograph (Shimadzu) equipped with an Aminex HPX-87

column (Bio-Rad) and a refractive index detector. Samples were centrifuged and filtered using FiltrEX filter 96-well plates (Corning).

## RESULTS AND DISCUSSION

**Growth with glucose.** We tested a possible means to complement the inability of *S. elongatus* to grow in the dark based on our hypothesis that efficient uptake of sugars is a missing factor for heterotrophy. Glucose is a common energy storage molecule in *S. elongatus* in the form of glycogen (24–27). Glycogen is built up within the cell throughout the light phase of metabolism and then used as an energy source to maintain essential chemical processes throughout the dark phase (26). Therefore, all the required genes for the breakdown of endogenous glucose ought to be present in *S. elongatus*. We installed three glucose transporter genes from a variety of organisms into the *S. elongatus* chromosome in an attempt to confer heterotrophic behavior under diurnal conditions (Fig. 1). These transporters include GlcP from *Synechocystis* sp. PCC 6803 (28), GalP from *Escherichia coli* (29), and Glut1 from human erythrocytes (30). Only the eukaryotic gene for Glut1 was codon optimized for *S. elongatus*. Each gene was integrated into the *S. elongatus* chromosome at neutral site I (NSI) under the control of an isopropyl- $\beta$ -D-1-thiogalactopyranoside (IPTG)-inducible promoter,  $P_{trc}$  (Fig. 1A) (22). Growth of the resulting three strains and the wild type was measured under diurnal illumination conditions in the presence and absence of glucose (Fig. 1B and C). To amplify the growth difference between strains that could and could not grow on extracellular glucose, conditions were set so as to limit the amount of  $\text{CO}_2$  (no bubbling) and light intensity (25  $\mu\text{E}/\text{m}^2/\text{s}$ ).

Throughout Results/Discussion, growth rate values reported from the light and dark cycles are derived from the 48-to-60-h and

TABLE 3 Installed genes in this study

Organism	Gene	Function
<i>E. coli</i> BW25113	<i>galP</i>	MFS-type D-galactose/ $\text{H}^+$ transporter
	<i>xylE</i>	MFS-type D-xylose/ $\text{H}^+$ transporter
	<i>xylA</i>	D-Xylose isomerase
	<i>xylB</i>	Xylulokinase
<i>Homo sapiens</i>	<i>GLUT1</i>	MFS-type D-glucose/ $\text{H}^+$ transporter
<i>Synechocystis</i> sp. PCC 6803	<i>glcP</i>	MFS-type D-glucose/ $\text{H}^+$ transporter
<i>E. coli</i> ATCC 700927	<i>cscB</i>	MFS-type D-sucrose/ $\text{H}^+$ transporter
	<i>cscK</i>	Fructokinase

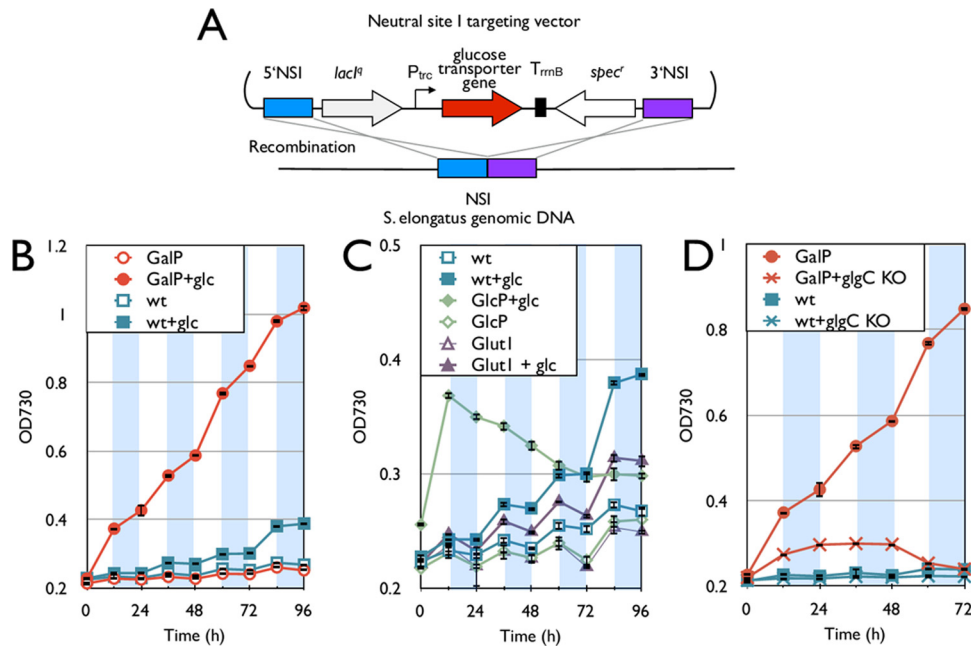


**FIG 1** Installation of glucose transporter to *S. elongatus*. (A) Schematic representation of glucose transporter gene integration into the *S. elongatus* genome. (B) Growth curve of the *galP* strain (red) and wild type (blue) with and without 5 g/liter glucose. (C) Growth curve of the *Glut1* (purple) and *glcP* (green) strains and the wild type. (D) Growth curve of the *galP* strain and the wild type with and without the *glgC* deletion (*glgC* KO). For panels B, C, and D, empty symbols are samples in BG-11 medium without glucose, while solid symbols indicate results with BG-11 containing 5 g/liter glucose. White and shaded areas indicate the light and dark cycles, respectively. All y axes denote  $OD_{730}$ , though the scales differ for visibility. Error bars represent standard deviations (in triplicate). NSI, neutral site 1.

60-to-72-h periods, respectively (growth rates for all periods, 0 to 96 h, are listed in Table 4). The baseline growth rate of wild-type *S. elongatus* based on the  $OD_{730}$  was  $0.161 \text{ day}^{-1}$  during the light cycle (48 h to 60 h) with no growth during the dark cycle (Fig. 1B and Table 4). The wild type grew at a higher rate ( $0.204 \text{ day}^{-1}$ ) when in the presence of glucose and light, yet exhibited no growth in the dark cycle (Fig. 1B). No changes in cellular morphology, such as size and shape of the cells grown with or without glucose,

were detected by microscopic observation (magnification, 1,000 $\times$ ). The only engineered strain to show a consistent increase in the growth rate in the presence of glucose contained *galP* (denoted as the *galP* strain) (Fig. 1B). In addition to increased growth compared to that of the wild type, the *galP* strain showed growth even during dark periods, whereas the wild type showed no growth (Fig. 1B and C). The growth rates of the *galP* strain under light and dark conditions in the presence of glucose were 0.540

**TABLE 4** Growth rates under diurnal conditions<sup>a</sup>

Strain	OE	KO	Sugar	Growth rate ( $\text{day}^{-1}$ ) for time period (h), condition							
				0–12, L	12–24, D	24–36, L	36–48, D	48–60, L	60–72, D	72–84, L	84–96, D
AL257				$0.082 \pm 0.064$	ND	$0.110 \pm 0.025$	ND	$0.161 \pm 0.030$	ND	$0.163 \pm 0.026$	ND
AL257			Glc	$0.128 \pm 0.008$	ND	$0.238 \pm 0.017$	ND	$0.204 \pm 0.018$	ND	$0.469 \pm 0.012$	ND
AL536		<i>glgC</i>	Glc	ND	ND	ND	ND	ND	ND	NA	NA
AL257			Suc	$0.298 \pm 0.010$	$0.081 \pm 0.007$	$0.319 \pm 0.015$	ND	$0.310 \pm 0.017$	$0.087 \pm 0.027$	$0.298 \pm 0.025$	$0.071 \pm 0.019$
AL257			Xyl	$0.149 \pm 0.021$	$0.104 \pm 0.017$	$0.285 \pm 0.012$	ND	$0.350 \pm 0.017$	$0.062 \pm 0.012$	$0.446 \pm 0.016$	$0.098 \pm 0.016$
AL361	<i>galP</i>			$0.128 \pm 0.017$	ND	$0.067 \pm 0.010$	ND	$0.126 \pm 0.018$	ND	$0.158 \pm 0.004$	ND
AL361	<i>galP</i>		Glc	$0.992 \pm 0.014$	$0.269 \pm 0.083$	$0.428 \pm 0.030$	$0.211 \pm 0.015$	$0.540 \pm 0.017$	$0.199 \pm 0.012$	$0.285 \pm 0.012$	$0.079 \pm 0.021$
AL535	<i>galP</i>	<i>glgC</i>	Glc	$0.438 \pm 0.016$	$0.159 \pm 0.013$	ND	ND	ND	ND	NA	NA
AL358	<i>glcP</i>			$0.122 \pm 0.025$	ND	$0.118 \pm 0.036$	ND	$0.112 \pm 0.040$	ND	$0.279 \pm 0.049$	ND
AL358	<i>glcP</i>		Glc	$0.730 \pm 0.008$	ND	ND	ND	ND	ND	ND	ND
AL360	<i>GLUT1</i>			$0.140 \pm 0.018$	ND	$0.112 \pm 0.014$	ND	$0.115 \pm 0.029$	ND	$0.292 \pm 0.045$	ND
AL360	<i>GLUT1</i>		Glc	$0.219 \pm 0.029$	ND	$0.212 \pm 0.027$	ND	$0.201 \pm 0.051$	ND	$0.352 \pm 0.055$	ND
AL1030	<i>cscKB</i>			$0.134 \pm 0.023$	ND	$0.106 \pm 0.032$	ND	$0.141 \pm 0.038$	ND	$0.148 \pm 0.026$	ND
AL1030	<i>cscKB</i>		Suc	$0.327 \pm 0.029$	$0.157 \pm 0.021$	$0.401 \pm 0.026$	$0.122 \pm 0.034$	$0.376 \pm 0.031$	$0.128 \pm 0.011$	$0.412 \pm 0.008$	$0.126 \pm 0.009$
AL1067	<i>xylE</i>			$0.102 \pm 0.004$	ND	$0.141 \pm 0.010$	ND	$0.161 \pm 0.020$	ND	$0.172 \pm 0.024$	ND
AL1067	<i>xylE</i>		Xyl	$0.140 \pm 0.021$	ND	$0.179 \pm 0.007$	ND	$0.154 \pm 0.015$	ND	$0.192 \pm 0.011$	ND
AL434	<i>xylEAB</i>			ND	ND	$0.050 \pm 0.011$	ND	$0.121 \pm 0.011$	ND	$0.106 \pm 0.014$	ND
AL434	<i>xylEAB</i>		Xyl	$0.395 \pm 0.026$	$0.351 \pm 0.014$	$0.572 \pm 0.025$	$0.336 \pm 0.012$	$0.471 \pm 0.012$	$0.291 \pm 0.020$	$0.313 \pm 0.015$	$0.082 \pm 0.020$

<sup>a</sup> These growth rates were calculated from the  $OD_{730}$  throughout diurnal conditions. All growth rates are the average rates for biological triplicates. The “ $\pm$ ” signs indicate standard deviations of rates, where  $n = 3$ . Any growth rate calculated to be less than  $0.050 \text{ day}^{-1}$  is considered insignificant and is shown here as not detectable (ND). AL257 is the wild type. L, light condition; D, dark condition; OE, overexpression; KO, deletion; Xyl, xylose; Glc, glucose; Suc, sucrose; NA, not analyzed.



day<sup>-1</sup> and 0.199 day<sup>-1</sup>, respectively. However, the glucose consumption of the *galP* strain after 96 h was not detectable with HPLC analysis. Calculations using OD<sub>730</sub> and cell counts predict the total change in dry biomass to be around 0.1 g/liter. Thus, using HPLC analysis, there was a high level of difficulty in detecting such a small change in the glucose concentration over a 96-h period while taking into account evaporation of water. The strain containing *glcP* showed increased growth (0.730 day<sup>-1</sup>) during the first light phase, but the growth stopped after that, which is consistent with the previous results (Fig. 1C) (4, 9). The strain containing *GLUT1* exhibited growth similar to that of the wild type (Fig. 1C). All growth assays were confirmed to be free of any significant contamination through microscopy and plating analyses upon completion (see Materials and Methods). These results demonstrate that *S. elongatus* can metabolize glucose for growth once it is transported into the cells. While each of these three heterologously expressed transporters is part of the major facilitator superfamily (MFS), each had a varied effect upon cell growth. We can assume these variations are related to the ability of these membrane proteins in *S. elongatus* to be adequately expressed, folded, and localized, as well as differences in enzymatic activity. Thus, the difficulty of predicting heterologous enzymatic activity, especially for membrane proteins, remains high.

Since *S. elongatus* naturally stores fixed carbon in the form of glycogen (31), it was hypothesized that some portion of the transported glucose was captured and stored instead of contributing to cell growth. To explore this possibility, a necessary gene for the formation of glycogen, *glgC*, was deleted from both the *galP* strain (denoted as the *galP-ΔglgC* strain) and the wild type (see Fig. S1 in the supplemental material). These strains were assayed to determine any change in growth behavior. The *galP-ΔglgC* strain failed to show any growth in the presence of glucose beyond the first light cycle (Fig. 1D). It has been shown that the deletion of *glgC* in the wild type also impaired growth (27), although the effects of *ΔglgC* in this study were larger than those reported previously (27). Further analysis will be required to elucidate the mechanism of the growth defect.

To characterize the expression of *galP* in *S. elongatus*, *gfp* was fused to the 3' end of *galP* (denoted as *galP-gfp*). The strains containing *galP-gfp* or *gfp* only were examined with fluorescent confocal microscopy (Fig. 2A and B). The strain containing *galP-gfp* showed a fluorescent signal only in the cellular membrane (Fig. 2B, right), while the *gfp*-containing control strain (AL504) (Table 1) showed a fluorescent signal throughout the cytoplasm (Fig. 2B, left), and the wild type did not show a fluorescent signal under these conditions (Fig. 2A). These results indicate that GalP from *E. coli* is successfully localized to the membrane of *S. elongatus* and may allow efficient transport of glucose into the cell.

Next, various concentrations of IPTG were added to the cultures of the *galP-gfp* strain, and the growth was measured under continuous-light conditions (Fig. 2C). The variation in IPTG concentrations led to a variation in growth rates of the cultures. This was also the case with the *galP*-containing strain, while the growth of the wild type was not altered with the addition of any amount of IPTG up to 1 mM. Optimum growth resulted from induction using 0.1 mM IPTG, while induction with a 1 mM concentration led to a slightly lower cell growth rate (Fig. 2C).

Fluorescence intensity of the cultures of the *galP-gfp* strain was measured throughout the growth assay (Fig. 2D). Time courses of GFP fluorescence intensity and the OD<sub>730</sub> of the *galP-gfp* strain

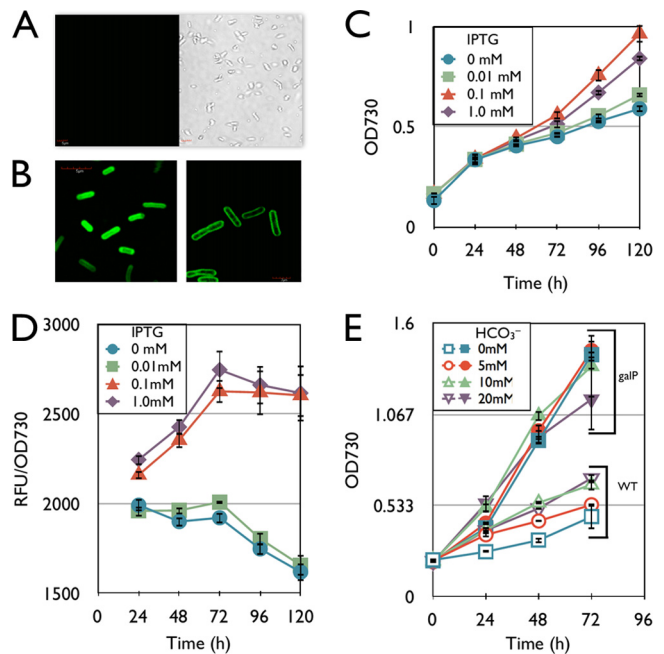
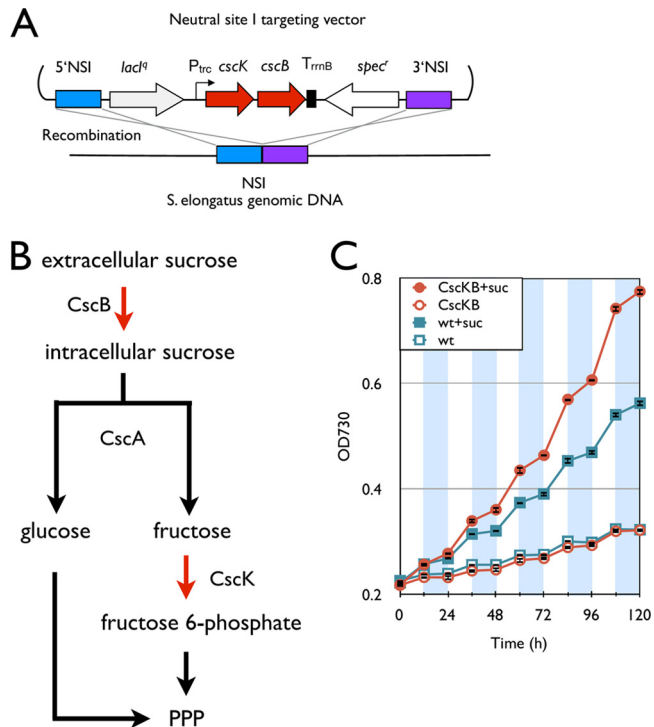


FIG 2 Characterization of the *galP* strain. All samples are grown in BG-11 medium with 5 g/liter glucose in continuous light. (A) Transmitted light (right) and confocal (left) images of the wild type. (B) Confocal microscope images of the *gfp* strain (left) and the *galP-gfp* strain (right). (C) Growth curve of the *galP-gfp* strain in the presence of various amounts of IPTG. (D) Fluorescence analysis of the *galP-gfp* strain during the course of the growth curve. The y axis indicates GFP fluorescence intensity divided by OD<sub>730</sub>. (E) Growth curve of the *galP* strain (without *gfp*) (filled symbols) and the wild type (open symbols) in the presence of various concentrations of sodium bicarbonate (NaHCO<sub>3</sub>). Error bars represent standard deviations (in triplicate).

were measured with various concentrations of IPTG (Fig. 2D). The standardized fluorescent intensity (relative fluorescence units [RFU]/OD<sub>730</sub>) indicated that 1 mM IPTG and 0.1 mM IPTG in the medium caused similar levels of expression of GalP-GFP, and expression from *P<sub>trc</sub>* was saturated with 0.1 mM IPTG for this construct.

The effects of bicarbonate on heterotrophic growth were characterized (Fig. 2E). This experiment was used to determine if heterotrophic growth of the *galP*-containing strain was measurable only due to the carbon limitations introduced by the assay conditions. The *galP* strain showed similar growth with or without various concentrations of bicarbonate- and glucose-containing medium in continuous light, while a higher concentration of bicarbonate slightly enhanced the growth of the wild type (Fig. 2E). The growth rate of the wild type increased to 0.398 day<sup>-1</sup> with 20 mM bicarbonate from 0.259 day<sup>-1</sup> without bicarbonate, while the growth rate of the *galP* strain did not change in the presence of bicarbonate (~0.636 day<sup>-1</sup>). These results suggest that carbon fixation is not the rate-limiting step for the growth of the *galP* strain in the presence of 5 g/liter glucose, while carbon fixation is growth limiting for the wild type under the same conditions. With the addition of bicarbonate in this experiment, the pH of the culture may increase as the bicarbonate is consumed. This basic pH may decrease sugar consumption by the H<sup>+</sup> symporter (7). Thus, it is important to maintain the pH of the culture around 7.0, at which the transport of sugars would be in the importing direction for efficient growth.



**FIG 3** Installation of the sucrose degradation pathway. (A) Schematic representation of integration of the sucrose degradation pathway into the *S. elongatus* chromosome. (B) Synthetic sucrose degradation pathway in *S. elongatus*. Red arrows indicate steps catalyzed by heterologous enzymes. PPP, pentose phosphate pathway. (C) Growth curves of the *cscB-cscK* strain (red) and the wild type (blue). Empty and filled symbols indicate growth without and with 5 g/liter sucrose, respectively. White and shaded areas indicate light and dark cycles, respectively. Error bars represent standard deviations (in triplicate).

**Growth with sucrose.** Sucrose is a natural metabolite in *S. elongatus*, and it has been shown to be synthesized in response to osmotic pressure (7, 27). The wild type with 5 g/liter sucrose had an increased growth rate,  $0.310 \text{ day}^{-1}$  and  $0.087 \text{ day}^{-1}$ , respectively, in the light and dark compared to the wild type without sucrose, at a rate of  $0.161 \text{ day}^{-1}$  and no growth in the light and dark, respectively (Fig. 3). This result shows that *S. elongatus* is weakly permeable to sucrose and can use sucrose as a carbon source. Seeking to improve these growth rates, a sucrose transporter gene and a fructokinase gene, *cscB* and *cscK*, respectively (*E. coli* ATCC 700927), were integrated into the *S. elongatus* genome (Fig. 3A). These genes were previously shown to be properly expressed in this organism (7). This strain was constructed to more fully allow sucrose into the cell through the CscB transporter and to be hydrolyzed to glucose and fructose by the endogenous sucrose invertase (putatively encoded by SYNPC7942\_0397). The fructokinase gene, *cscK*, was overexpressed to maximize the carbon flux to fructose-6-phosphate, a central metabolite in the oxidative pentose phosphate pathway (32). It was found that the *cscK-cscB* strain had increased growth rates,  $0.376 \text{ day}^{-1}$  (light) and  $0.128 \text{ day}^{-1}$  (dark), in the presences of 5 g/liter sucrose (Fig. 3C). Although sucrose enhanced the growth of the wild type, the effects of sucrose were larger in the *cscB-cscK* strain than in the wild type.

**Growth with xylose.** Xylose is the major part of abundantly

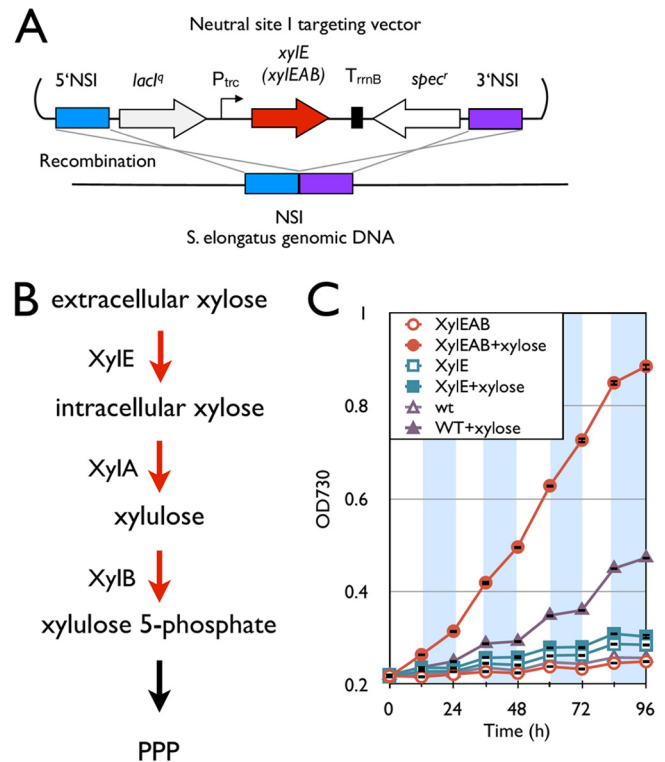


**FIG 4** Installation of the xylose degradation pathway. (A) Schematic representation of integration of the xylose degradation pathway into the *S. elongatus* chromosome. (B) Synthetic xylose degradation pathway in *S. elongatus*. Red arrows indicate steps catalyzed by heterologous enzymes. (C) Growth curves of the *xylE* and *xylEAB* strains and the wild type. Empty and filled symbols indicate growth without and with 5 g/liter xylose, respectively. White and shaded areas indicate light and dark cycles. Error bars represent standard deviations (in triplicate).

available hemicellulosic materials and may be a promising inexpensive renewable feedstock for microbial production of biofuels and chemicals (33). Importantly, xylose is not a known metabolite of *S. elongatus*. To engineer *S. elongatus* so that it can utilize xylose, *xylE*, encoding a xylose transporter, from *E. coli* was integrated into *S. elongatus* (Fig. 4A). However, the xylose transporter not only failed to improve the growth of the strain in the presence of xylose under diurnal conditions, but this mutant had a significantly reduced growth rate ( $0.154 \pm 0.015$ ) compared to that of the wild type ( $0.350 \pm 0.017$ ) (Fig. 4C). Since xylose slightly improved the growth of the wild type (Fig. 4C), *S. elongatus* seems to be able to consume xylose slowly. However, the expression of *xylE* may greatly increase the amount of xylose accumulated within the cell owing to its slow metabolism, causing a metabolic imbalance. Thus, we hypothesized that some downstream enzymes for converting xylose to central metabolites efficiently are missing. We searched the *S. elongatus* genome sequence and found that the *S. elongatus* genome is not known to contain homologs of *xylA* and *xylB*, encoding xylose isomerase and xylulokinase, respectively. Xylose isomerase and xylulokinase are responsible for the first two steps of xylose degradation (Fig. 4B). To introduce xylose isomerase and xylulokinase into *S. elongatus*, an operon including *xylE*, *xylA*, and *xylB* from *E. coli* was integrated into the *S. elongatus* genome (denoted as the *xylEAB* strain) (Fig. 4A). This strain was shown to have a much higher heterotrophic growth rate under

diurnal conditions than the wild type (Fig. 4C). This operon also allowed heterotrophic growth in the dark part of diurnal conditions, while the wild-type growth rate was marginal (Fig. 4C). The *xylEAB* strain had growth rates of  $0.471 \text{ day}^{-1}$  and  $0.291 \text{ day}^{-1}$  in the light and dark, respectively, in the presence of xylose. This is in contrast to the wild-type growth rates of  $0.350 \text{ day}^{-1}$  and  $0.062 \text{ day}^{-1}$  under the same conditions. The xylose consumption rate was measured by HPLC to average about  $10 \text{ mg h}^{-1}$  over the 96-h growth period. Interestingly, the maximum growth of the *galP* strain ( $0.992 \pm 0.014$ ) was faster than that of the *xylEAB* strain ( $0.572 \pm 0.025$ ) under the light condition in the presence of their respective sugars owing to rapid growth in the *galP* strain in the first 12 h (Fig. 1B and 4C). After the initial 12 h, the growth rates of the two strains were comparable in the light. However, the maximum growth in the dark of the *xylEAB* strain ( $0.351 \pm 0.014$ ) was faster than that of the *galP* strain ( $0.269 \pm 0.083$ ) in the presence of their respective sugars (Fig. 1B and 4C).

We have successfully engineered *S. elongatus* so that it can grow continuously under diurnal conditions by using common fixed carbon sources for growth. In general, heterotrophic cyanobacteria utilize relatively few substrates for the buildup of biomass (18). The well-known photoheterotrophic cyanobacterium *Synechocystis* sp. 6803 can utilize glucose under photomixotrophic conditions of growth, with a reported growth rate of  $1.38 (\text{day}^{-1})$  (34). This is slightly faster than the fastest growth shown here for the *galP* strain under photomixotrophic conditions, with a growth rate of about  $0.99 (\text{day}^{-1})$ . However, *Synechocystis* sp. 6803 has not been shown to consume xylose, demonstrating the versatile nature of this synthetic sugar transporter strategy. Sugar transporters, as well as other peripheral genes, were integrated for the increased growth rate of a model photoautotrophic cyanobacterium under both light and dark conditions. While the particular genes necessary for each specific feedstock may differ, these results suggest that the cause of autotrophy in this organism lies within the peripheral metabolic processes. Core catabolic pathways for common sugar utilization seem to be functional in *S. elongatus*.

Cyanobacteria are increasingly being studied for the production of valuable natural products, as well as biofuels and chemicals (35). Optimal industrial conditions must be explored in order to maximize productivity and lead to efficient utilization of resources to remain competitive. In order for any cyanobacterial chemical production to be economically competitive, the light energy must be supplied from the sun, a natural diurnal condition, with production possible for only a portion of the day. To improve this production scenario, the development of heterotrophic and/or mixotrophic growth conditions that utilize diverse feedstocks and production processes applicable to a major category of cyanobacteria is desirable. Additionally, even under light conditions, photoautotrophic growth is often limited by light deficiency due to mutual shading of cells. As a result, the overall productivity of a photoautotrophic system is low. In this work, we developed a strategy to allow growth of an obligate photoautotroph on diverse feedstocks. As such, this example of modification of an obligate photoautotroph for continuous growth under diurnal conditions demonstrates key advantages of using a synthetic biological approach to expand the natural feedstocks of a particular class of organisms.

In this work, we examined the growth behavior of engineered *S. elongatus* under diurnal conditions. We have determined one underlying cause of natural photoautotrophy in this bacterium by

engineering the organism to allow diurnal growth. For complete organoheterotrophic conversion of *S. elongatus*, the strain must be able to grow in the complete absence of light. In future work, we will seek to engineer the strains from this work to allow growth under continuously dark conditions. The activities of all photosynthetic organisms are energy intensive, interconnected with central metabolism, and are strictly regulated according to light intensity. The activity of these reactions will sharply decrease once exposure to light ceases, although the fixation of  $\text{CO}_2$  has been observed up to 8 h into the dark cycle during diurnal conditions (36). In *S. elongatus*, light regulation takes place through two major routes: transcriptional and posttranslational. Each of these regulatory pathways uses the redox state of the electron transport chain as a way of sensing the light conditions (37, 38), transducing this signal through various mediator systems, such as KaiABC and the ferredoxin/thioredoxin system (37, 39–41). We anticipate the need to decouple this regulation through continued metabolic engineering. Another possibility is exploring a light pulsing strategy similar to the light-activated heterotrophic growth seen in *Synechocystis* sp. strain PCC 6803 (42). While diurnal conditions are of keen interest for cost-effective, industrial pursuits, further work with continuously dark conditions will more fully illuminate the causes of phototrophy seen in this model cyanobacterium.

## ACKNOWLEDGMENTS

This study was supported by a National Science Foundation grant (1132442).

We thank Gang-Yu Liu and Jie-Ren Li for assistance with confocal microscopy in the UCD NEAT Spectral Imaging Facility, John C. Meeks, J. Clark Lagarias, and Christine A. Rabinovitch-Deere for helpful comments on the manuscript, and Noeli Acoba for experimental assistance.

## REFERENCES

- Chen GQ, Chen F. 2006. Growing phototrophic cells without light. *Biotechnol. Lett.* 28:607–616.
- Wood AP, Aurikko JP, Kelly DP. 2004. A challenge for 21st century molecular biology and biochemistry: what are the causes of obligate autotrophy and methanotrophy? *FEMS Microbiol. Rev.* 28:335–352.
- Zaslavskaja LA, Lippmeier JC, Shih C, Ehrhardt D, Grossman AR, Apt KE. 2001. Trophic conversion of an obligate photoautotrophic organism through metabolic engineering. *Science* 292:2073–2075.
- Zhang C-C, Jeanjean R, Joset F. 1998. Obligate phototrophy in cyanobacteria: more than a lack of sugar transport. *FEMS Microbiol. Lett.* 161:285–292.
- Cogne G, Gros JB, Dussap CG. 2003. Identification of a metabolic network structure representative of *Arthrospira* (*Spirulina*) *platensis* metabolism. *Biotechnol. Bioeng.* 84:667–676.
- Zhang S, Bryant DA. 2011. The tricarboxylic acid cycle in cyanobacteria. *Science* 334:1551–1553.
- Ducat DC, Avelar-Rivas JA, Way JC, Silver PA. 2012. Rerouting carbon flux to enhance photosynthetic productivity. *Appl. Environ. Microbiol.* 78:2660–2668.
- Niederholtmeyer H, Wolfstadter BT, Savage DF, Silver PA, Way JC. 2010. Engineering cyanobacteria to synthesize and export hydrophilic products. *Appl. Environ. Microbiol.* 76:3462–3466.
- Stebegg R, Wurzinger B, Mikulic M, Schmetterer G. 2012. Chemoheterotrophic growth of the cyanobacterium *Anabaena* sp. strain PCC 7120 dependent on a functional cytochrome *c* oxidase. *J. Bacteriol.* 194:4601–4607.
- Ungerer JL, Pratte BS, Thiel T. 2008. Regulation of fructose transport and its effect on fructose toxicity in *Anabaena* spp. *J. Bacteriol.* 190:8115–8125.
- Wargacki AJ, Leonard E, Win MN, Regitsky DD, Santos CNS, Kim PB, Cooper SR, Raisner RM, Herman A, Sivitz AB, Lakshmanaswamy A, Kashiya Y, Baker D, Yoshikuni Y. 2012. An engineered microbial platform for direct biofuel production from brown macroalgae. *Science* 335:308–313.



12. Atsumi S, Higashide W, Liao JC. 2009. Direct photosynthetic recycling of carbon dioxide to isobutyraldehyde. *Nat. Biotechnol.* 27:1177–1180.
13. Liu X, Fallon S, Sheng J, Curtiss R, III. 2011. CO<sub>2</sub>-limitation-inducible green recovery of fatty acids from cyanobacterial biomass. *Proc. Natl. Acad. Sci. U. S. A.* 108:6905–6908.
14. Liu X, Sheng J, Curtiss R, III. 2011. Fatty acid production in genetically modified cyanobacteria. *Proc. Natl. Acad. Sci. U. S. A.* 108:6899–6904.
15. Machado IMP, Atsumi S. 2012. Cyanobacterial biofuel production. *J. Biotechnol.* 162:50–56.
16. Robertson D, Jacobson S, Morgan F, Berry D, Church G, Afeyan N. 2011. A new dawn for industrial photosynthesis. *Photosynth. Res.* 107:269–277.
17. Tan LT. 2007. Bioactive natural products from marine cyanobacteria for drug discovery. *Phytochemistry.* 68:954–979.
18. Rippka R, Deruelles J, Waterbury JB, Herdman M, Stanier RY. 1979. Generic assignments, strain histories and properties of pure cultures of cyanobacteria. *J. Gen. Microbiol.* 111:1–61.
19. Atsumi S, Hanai T, Liao JC. 2008. Non-fermentative pathways for synthesis of branched-chain higher alcohols as biofuels. *Nature* 451:86–89.
20. Ivleva NB, Bramlett MR, Lindahl PA, Golden SS. 2005. LdpA: a component of the circadian clock senses redox state of the cell. *EMBO J.* 24:1202–1210.
21. Kovach ME, Phillips RW, Elzer PH, Roop RM, II, Peterson KM. 1994. pBBR1MCS: a broad-host-range cloning vector. *Biotechniques* 16:800–802.
22. Golden S, Brusslan J, Haselkorn R. 1987. Genetic engineering of the cyanobacterial chromosome. *Methods Enzymol.* 153:215–246.
23. Bustos SA, Golden SS. 1991. Expression of the *psbDII* gene in *Synechococcus* sp. strain PCC 7942 requires sequences downstream of the transcription start site. *J. Bacteriol.* 173:7525–7533.
24. Ball SG, Morell MK. 2003. From bacterial glycogen to starch: understanding the biogenesis of the plant starch granule. *Annu. Rev. Plant Biol.* 54:207–233.
25. Preiss J. 1984. Bacterial glycogen synthesis and its regulation. *Annu. Rev. Microbiol.* 38:419–458.
26. Smith AJ. 1983. Modes of cyanobacterial carbon metabolism. *Ann. Microbiol. (Paris)* 134B:93–113.
27. Suzuki E, Ohkawa H, Moriya K, Matsubara T, Nagaike Y, Iwasaki I, Fujiwara S, Tsuzuki M, Nakamura Y. 2010. Carbohydrate metabolism in mutants of the cyanobacterium *Synechococcus elongatus* PCC 7942 defective in glycogen synthesis. *Appl. Environ. Microbiol.* 76:3153–3159.
28. Zhang CC, Durand MC, Jeanjean R, Joset F. 1989. Molecular and genetical analysis of the fructose-glucose transport system in the cyanobacterium *Synechocystis* PCC6803. *Mol. Microbiol.* 3:1221–1229.
29. Hernandez-Montalvo V, Martinez A, Hernandez-Chavez G, Bolivar F, Valle F, Gosset G. 2003. Expression of *galP* and *glk* in a *Escherichia coli* PTS mutant restores glucose transport and increases glycolytic flux to fermentation products. *Biotechnol. Bioeng.* 83:687–694.
30. Mueckler M, Caruso C, Baldwin SA, Panico M, Blench I, Morris HR, Allard WJ, Lienhard GE, Lodish HF. 1985. Sequence and structure of a human glucose transporter. *Science* 229:941–945.
31. Stanier RY. 1975. The utilization of organic substrates by cyanobacteria. *Biochem. Soc. Trans.* 3:352–359.
32. Bassham JA, Benson AA, Calvin M. 1950. The path of carbon in photosynthesis. *J. Biol. Chem.* 185:781–787.
33. Steen EJ, Kang Y, Bokinsky G, Hu Z, Schirmer A, McClure A, Del Cardayre SB, Keasling JD. 2010. Microbial production of fatty-acid-derived fuels and chemicals from plant biomass. *Nature* 463:559–562.
34. Vermaas W. 1996. Molecular genetics of the cyanobacterium *Synechocystis* sp. PCC 6803: principles and possible biotechnology applications. *J. Appl. Phycol.* 8:263–273.
35. McEwen JT, Atsumi S. 2012. Alternative biofuel production in non-natural hosts. *Curr. Opin. Biotechnol.* 23:744–750.
36. Paul JH, Kang JB, Tabita FR. 2000. Diel patterns of regulation of *rbcl* transcription in a cyanobacterium and a prymnesiophyte. *Mar. Biotechnol. (NY)* 2:429–436.
37. Buchanan BB, Balmer Y. 2005. Redox regulation: a broadening horizon. *Annu. Rev. Plant Biol.* 56:187–220.
38. Golden SS. 1995. Light-responsive gene expression in cyanobacteria. *J. Bacteriol.* 177:1651–1654.
39. Ivleva NB, Gao T, LiWang AC, Golden SS. 2006. Quinone sensing by the circadian input kinase of the cyanobacterial circadian clock. *Proc. Natl. Acad. Sci. U. S. A.* 103:17468–17473.
40. Lindahl M, Florencio FJ. 2003. Thioredoxin-linked processes in cyanobacteria are as numerous as in chloroplasts, but targets are different. *Proc. Natl. Acad. Sci. U. S. A.* 100:16107–16112.
41. Schmitz O, Katayama M, Williams SB, Kondo T, Golden SS. 2000. CikA, a bacteriophytochrome that resets the cyanobacterial circadian clock. *Science* 289:765–768.
42. Anderson SL, McIntosh L. 1991. Light-activated heterotrophic growth of the cyanobacterium *Synechocystis* sp. strain PCC 6803: a blue-light-requiring process. *J. Bacteriol.* 173:2761–2767.